Article

Separation of VOC Gaseous Mixtures Using an Adsorption–Desorption Device

Ľudmila Gabrišová [1], Oliver Macho [1,*], Martin Juriga [1], Zuzana Gábrišová [2], Ivan Valent [3], Juraj Kabát [4], Jaroslav Blaško [4] and Róbert Kubinec [4]

[1] Institute of Process Engineering, Faculty of Mechanical Engineering, Slovak University of Technology in Bratislava, Námestie Slobody 17, 812 31 Bratislava, Slovakia; ludmila.gabrisova@stuba.sk (Ľ.G.)

[2] Institute of Technologies and Materials, Faculty of Mechanical Engineering, Slovak University of Technology in Bratislava, Námestie Slobody 17, 812 31 Bratislava, Slovakia

[3] Department of Physical and Theoretical Chemistry, Faculty of Natural Sciences, Comenius University in Bratislava, Ilkovičova 6, 842 15 Bratislava, Slovakia

[4] Department of Analytical Chemistry, Faculty of Natural Sciences, Comenius University in Bratislava, Ilkovičova 6, 842 15 Bratislava, Slovakia

* Correspondence: oliver.macho@stuba.sk; Tel.: +421-2-57296-529

Abstract: The aim of this work was to separate ethanol in an experimental adsorption–desorption device. We focused on concentrating ethanol by adsorption onto granulated activated carbon in its gaseous phase, which was produced by stripping a matrix with different ethanol concentrations (2, 5, 10, and 15% v/v). For adsorption, three kinds of granulated activated carbon (GAC) were used, marked as GAC1, GAC2, and GAC3. The separation product had a higher ethanol concentration than the initial ethanol concentration before the adsorption–desorption process. The enrichment factor was, in the case of the initial ethanol concentration, 2% v/v at the level of 10. With our new adsorption–desorption device, it is possible to achieve a product with an ethanol concentration of 59.0% v/v with stripping, adsorption, desorption, and condensation. To verify the separation efficiency, a real matrix (fermentation broth) was used. The ethanol concentration in the real matrix was, at the beginning of the separation process, 0.65% v/v; after using our separation device, it was 11.35% v/v. Using a real matrix, the enrichment factor was at the level of 18. The main advantage is the use of our new adsorption–desorption device for the continuous separation of ethanol from fermentation broth. A mathematical model was created, based on which it is possible to calculate the ethanol concentration in the product of the separation process with high accuracy.

Keywords: ethanol; adsorption; desorption; stripping; granulated activated carbon

1. Introduction

At present, there are many methods for the separation of volatile organic compounds (VOCs) based on adsorption–desorption processes, but it is necessary to look at them in terms of the overall environmental impact, sustainability, and efficiency. VOC separation methods are often based on principles that have been known for a long time, and they can be divided into two groups. The separation techniques can be classified as recovery techniques and destruction techniques. In the group of recovery techniques, we can find adsorption, desorption, stripping, membrane filtration, etc., but achieving efficiency using these processes, in many ways, can be difficult [1,2]. Each technological approach must consider several factors; in addition to yield, there are financial factors, recycling factors, life cycle factors, etc. [3]. Adsorption techniques [4] have many advantages: they are nondestructive and effective for both VOC enrichment and separation. Adsorbed compounds can be desorbed by local increases in temperature or decreases in pressure [5–8]. An important feature that provides adsorbents with an industrial advantage is their repeatable usability, operating cost, and safety. The most used adsorbents includes activated carbon, zeolites,

resins, and metal–organic frameworks [2,6,9]. In our study, we focused on granulated activated carbon (GAC), which is, for our purpose, the best form of activated carbon. GAC was chosen for its affordability; compared to polymer resins and MOFs, GAC is much cheaper and more readily available on the market. Zeolites are comparable in price, but based on the available literature, we found that GAC often has the upper hand in terms of adsorption capacity and selectivity [10,11]. GACs are materials that are characteristic for their high specific surface area, high adsorption capacity, and simple manipulation, and they are suitable for use with a wide range of pHs [12]. GACs are affordable and reusable [13,14]. The surface of GACs can be modified using various approaches so that they meet the requirements of the separation process (increasing/reducing hydrophobicity) [15–17]. A crucial factor in the separation of compounds using GAC is the presence of functional groups on the surface (oxygen, nitrogen, or sulfur functional groups) [18–21]. A more difficult situation occurs if the nature of the separated compounds is the same (in terms of polarity and hydrophobicity), resulting in competition regarding the occupation of active sites on the surface of the adsorbent [6,22–27]. Such cases occur, for example, in the separation of compounds produced by fermentation [28]. Fermentation is the process in which ethanol is obtained from sugars through the fermentation of the yeast *Saccharomyces cerevisiae* [1,29–31]. However, in addition to ethanol, other compounds with the same polarity are also formed, and all this takes place in aqueous media. A matrix of this nature struggles in ethanol separation; therefore, these compounds' different volatilities are one of the decisive factors [29,32–34]. The main reason for recovering ethanol from the fermentation broth is product inhibition [35]. The ethanol concentration that acts as an inhibitor occurs at the level of 11–12 w% [25] or 6–10% depending on the microorganism [36,37]. In many cases, however, this is a question of the value of the concentration, and this is what we focused on in our research when separating ethanol. The uniqueness of this device lies in the fact that the separation process takes place in a closed cycle, which makes it possible to ensure a continuous process of the formation and separation of ethanol in the fermentation broth. Available research based on the same separation processes does not work with a closed cycle provided by an air blower. In these works, pressure cylinders with gases (air, CO_2, or nitrogen) are used for stripping [31,35,38]. Our separation device works in a closed cycle, and the separation of ethanol from the matrix (stock solution or fermentation broth) takes place at a laboratory temperature.

2. Materials and Methods

Ethanol nondenaturated p.a. (96%) was purchased from Centralchem (Bratislava, Slovakia). Granulated activated carbon GAC1 was purchased from PGChem (Nové Zámky, Slovakia), and GAC2, and GAC3 were purchased from SandSystem (Ostrava, Czech Republic). An experimental setup is shown in Figure 1. Mass transfer proceeds in the direction of the arrows and is provided by air blower, as shown in Figure 1. A preliminary study and complete separation process in a new adsorption–desorption device are described in our previous study [39]. The principle of the separation process in our device is simple and can be described as follows: each experiment is provided in a closed cycle, which is carried out by an air-blower. Air from the air-blower is blown into the stock vessel with an ethanol–water mixture (stock solution (SS)) with different ethanol concentrations (2, 5, 10, and 15% *v/v*); the airflow was set to 5 L/min. The SS is stripped by air from the air-blower and the created gaseous phase (adsorbate) is transferred to the adsorption bed. The adsorption bed is filled with 80 g of GAC with moisture at max. 2%. An adsorbate, gaseous phase (water vapor and ethanol) is adsorbed onto GAC until the adsorption bed is saturated. The stripping and adsorption take place at laboratory temperature. The ethanol concentration in SS and gaseous phase decrease until GAC is saturated; when this point is reached, the adsorption is stopped, and the next phase is desorption with continuous condensation. The desorption takes place at 120 °C, so the molecules of adsorbate are desorbed by high temperatures and, after desorption, are transported into the condenser, where they condense at 5–6 °C. The product of the separation process is a condensate with

a higher ethanol concentration than that in SS. The ethanol concentration in SS (before and after the separation process) and in the separation product is calculated from the density. The density of these mixtures is determined using the digital density meter DMA 48, Anton Paar (Graz, Austria). The calculation of the ethanol concentration from density is based on table density values related to temperature from Handbook Perry [40]. The time of the adsorption and desorption was determined experimentally. Adsorption took place for 8 h and desorption for 1 h. After conducting a series of experiments to determine the efficiency of the ethanol separation, an adsorption–desorption device was used for the ethanol separation with a real matrix–fermentation broth. The process parameters of the experiments with the real matrix were the same as during the experiments with the ethanol–water mixtures. Each of the experiments was repeated 3 times.
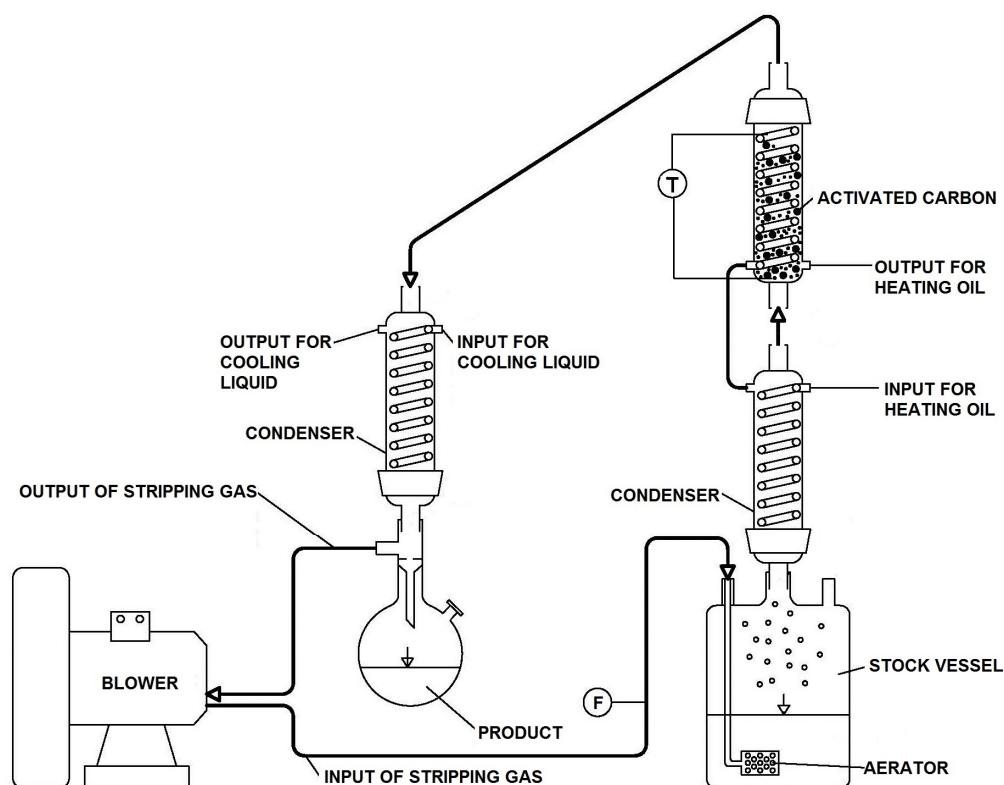

Figure 1. Scheme of a new adsorption–desorption device. F: flow meter; T: location of thermocouples.

2.1. Analysis of Gas Samples by GC-FID

For the determination of ethanol concentration, GC-FID 8890 gas chromatograph from Agilent Technologies (Santa Clara, CA, USA) was used. For an analysis of the ethanol concentration in the device, a gas proof syringe (Agilent Technologies) with a total volume of 500 μL was used. The gaseous phase, which was created by stripping the SS (before adsorption bed/adsorption), and the gaseous phase behind the adsorption bed (after adsorption) were sampled for analysis. For the analysis, 200 μL of gas with ethanol content was injected with a split ratio of 150:1 and split flow of 225 mL/min. The inlet temperature was set at 250 °C. For the sample GC-FID separation, a capillary column HP-5 (30.0 m × 320.0 μm × 0.25 μm, Agilent Technologies) was used, and the oven temperature was set to 40 °C, with a hold time of 4 min.

2.2. Analysis of Liquid Samples Using GC-FID

For the determination of the ethanol concentration in the fermentation broth and the separation product, the gas chromatograph GC-FID 6850 (Agilent Technologies) was used. The conditions for the analysis were as follows: column SPB-1 30.0 m × 320.0 μm × 0.25 μm. The initial temperature was set at 60 °C with a temperature gradient of 20 °C/min, with

a final temperature of 310 °C and a hold time of 4 min. For the analysis, a split mode was used with a ratio of 15:1; the volume of the injected sample was 0.2 µL, and the flow of carrier gas was 1.7 mL/min. For the calibration curve of the ethanol, 96% ethanol was purchased from Centralchem (Bratislava, Slovakia). For the determination of the glucose, fructose, and saccharose, standards purchased from Sigma Aldrich (Saint-Louis, MO, USA) were used. For the derivatization of all observed sugar components as derivative agents, 1,1,1,3,3,3-hexamethyldisilazane (HMDS); *N,O*-bis(trimethylsilyl)trifluoroacetamide (BSTFA); trifluoroacetic acid purchased from Fluorochem (Hadfield, UK, GB); and acetonitrile (ACN) purchased from Fluorochem (GB) were used.

Sample Preparation

A total of 300 µL ACN, 300 µL HMDS, and 2.5 µL TFA were added to 5 µL of the sample, and the content of the opened vial was shaken with a thermo-shaker at 50 °C for 30 min. After 30 min, 400 µL BSTFA was added, and the sample was shaken in a closed vial for 30 min at 80 °C. Derivatized samples were centrifuged, and the supernatant was separated for chromatographic analysis.

2.3. Theoretical Background of Ethanol Content

First, it is important to calculate a molar fraction of ethanol and water in the liquid (stock solution) x_i. For this purpose, we used the formula for molar faction calculation, which is described as Equation (1):

$$x_i = \frac{n_i}{n_{total}}, \tag{1}$$

where x_i is the molar fraction of component i, n_i is the amount of substance of the component i, and n_{total} is the sum of the amount of substances in the system. For the ethanol content in the gaseous phase, mathematical calculations were based on Raoult's law [41], as in Equation (2):

$$p_i = x_i \times p_i^\circ, \tag{2}$$

where p_i is the partial pressure of component i in the gaseous mixture, and p_i° is the vapor pressure of component i in the pure gas state.

For a molar fraction of component i in the gaseous phase, the formula described in Equation (3) can be used:

$$y_i = \frac{p_i}{p_{total}}, \tag{3}$$

where y_i is a molar fraction of component i in a gaseous phase, and p_{total} is the sum of all partial pressures of the compounds present in the system.

According to the formulas mentioned above, Equation (4) applies:

$$\frac{y_i}{y_{i+1}} = \frac{p_i}{p_{i+1}}, \tag{4}$$

where y_{i+1} and p_{i+1} presents the molar fraction of another component in the system and the partial pressure of the other component in the system, respectively.

The results of the molar fraction calculations related to the volume fraction of the experimental solutions (SS) are shown in the graph in Figure 2. From the graph, it is clear that values of the molar fraction in the gaseous state are higher than values of the molar fraction in liquids [42]. The results of our calculations of molar fractions correspond with the results of the publication by Waller and Strang [43].
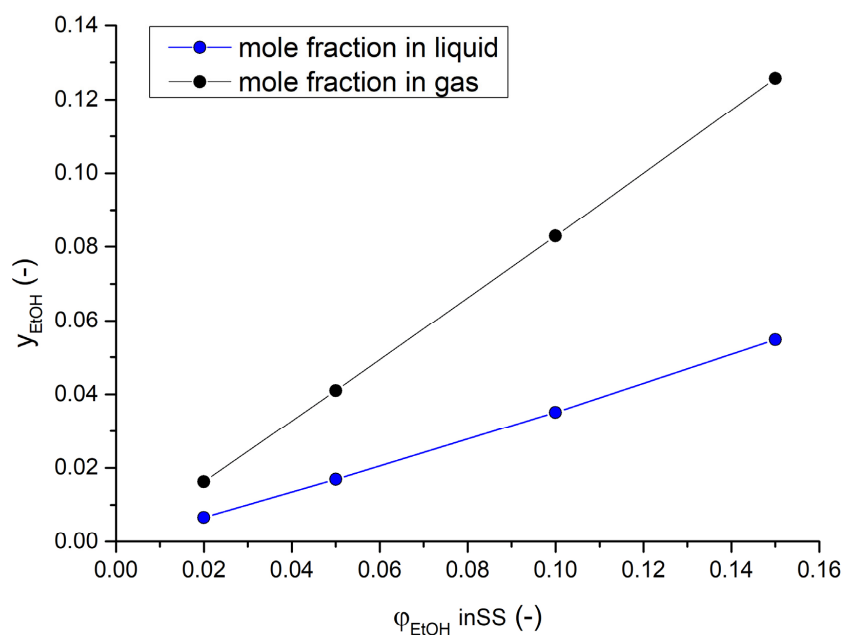
Figure 2. Graph of the molar fraction of ethanol in liquid phase and gas phase comparison at 25 °C.

3. Results and Discussion

3.1. Characterization of GAC

The particle size distribution is a parameter that affects the flow of the gases. This parameter can create resistance during the separation process, which negatively affects media transfer. To determine the resistance effect of the gas flow mixture, the particle size distribution measurement of all three types of GAC was provided by PartAn 3D particle and shape analyzer from Microtrac (Haan, Germany). The GAC particles were characterized volumetrically in agreement with ISO standards (13322-2 [44], 9276-6 [45]). The mean particle size (mm) of the area equivalent diameters was selected as a characteristic dimension determining the size of individual samples. The results of the analysis are shown in Figure 3, where it is clear that all three GACs had a uniform particle size distribution, and so this parameter would affect the gas flow in each experiment the same amount. The highest fraction in the analyzed samples of GAC had particles with a size between 2 and 3 mm. During the experiments, no consolidation of the GAC particles was observed, so the medium transfer was not affected by this phenomenon [24].
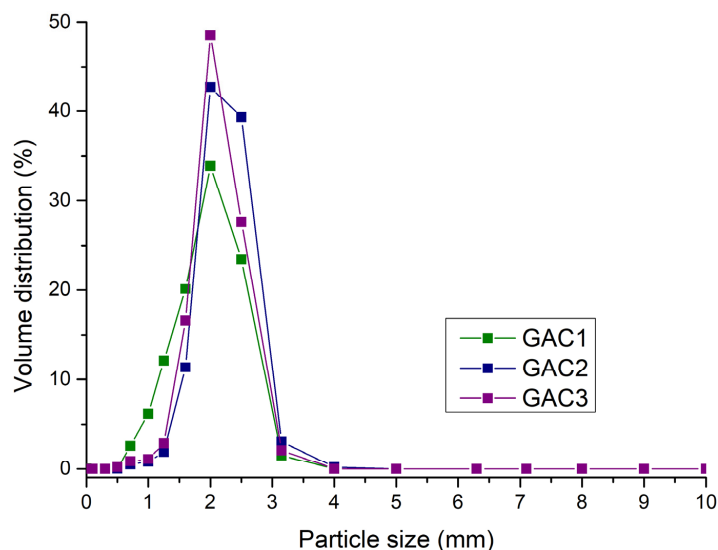

Figure 3. The particle size distribution of GACs analyzed uisng PartAn 3D.

The surface analysis of the elements was realized using a JEOL JSM IT300 LV scan electron microscope (SEM) with an EDS analyzer Oxford Instruments X-Max (Tokyo, Japan). This method is commonly used for the surface characterization of adsorbents [3,32,46–48]. The GACs' element surface composition was analyzed using SEM, and the captured pictures are shown in Figure 4. The characterization of GAC with SEM was carried out to determine the content of heterogeneous atoms on the surface of GACs (O, N, P, and S) and the complexity of the surface structure of activated carbon. The GACs' surface area was determined with a Surfer gas adsorption porosimeter by Thermo Scientific (Waltham, MA, USA). The adsorption and desorption isotherm measurements took place at the temperature of liquid nitrogen (77.4 K). According to [49–51], a common method to determine the surface area is with subcritical fluids such as liquid nitrogen. The surface area was calculated using the BET. method. The BET method considers the multilayer adsorption of the adsorbate onto GAC. The BET isotherm is an extension of the Langmuir isotherm. The principle of BET isotherms is that, even at low pressures (before surface saturation), polymolecular layers can form on the surface of the adsorbent. If we consider that the entire surface is composed of partial surfaces $a_0 \ldots a_i$, then each of them can be covered with $1 \ldots i$ layers. Adsorbents such as GAC are characterized by an IV-type adsorption isotherm. The isotherms GAC1–GAC3, determined using Surfer, had the same type. The pore size was calculated with the BJH method [52]. The preparation of the GACs for the surface area determination took 4 h at a temperature of 350 °C. The adsorption phase for determining the surface area lasted 6 h. The desorption of the adsorbed nitrogen lasted 3 h. The physical parameters obtained using the electron microscope and gas porosimeter are summarized in Table 1.
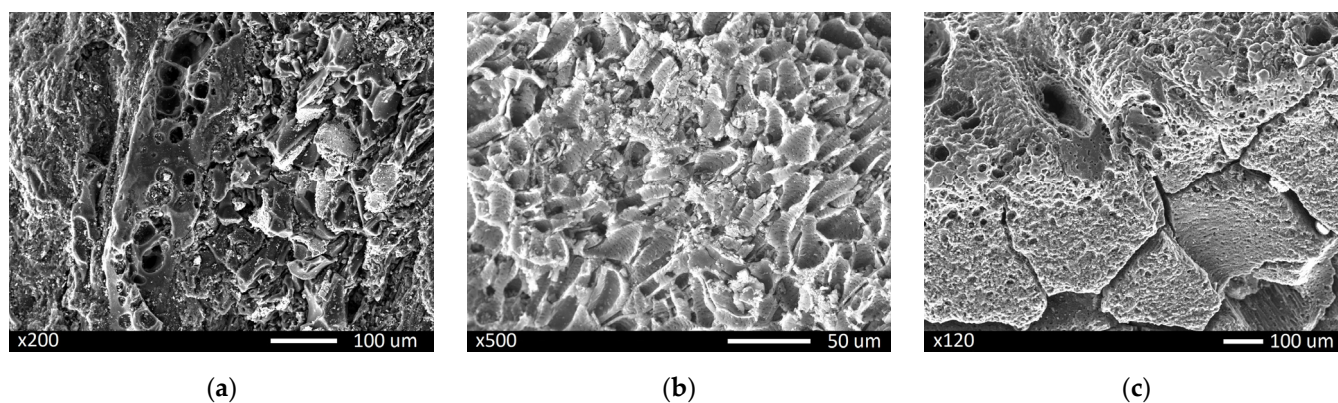

(a) (b) (c)

Figure 4. SEM pictures of the GACs' detailed surfaces: (**a**) GAC1; (**b**) GAC2; (**c**) GAC3.

Table 1. The physical properties of GACs analyzed using a SEM JOEL and Surfer gas adsorption porosimeter.

Type GAC	SA (m^2/g)	O (%)	C (%)	V_p (cm^3/g)	r_p (nm)
GAC1	736.12	0	98.6	0.524	1.721
GAC2	927.23	3.8	95.4	0.575	1.652
GAC3	1025.97	5.7	92.5	0.626	1.769

From the results, as shown in Table 1, it is clear that the surfaces of the chosen GACs are highly structuralized and porous, as indicated by the specific surface values obtained through the Surfer analysis. An elemental analysis of the GACs' surface showed variability in the oxygen content, which can play a significant role in VOC adsorption. On the GAC, the primary oxygen functional group accountable for the sorption of ethanol and other polar molecules is typically the carbonyl group (C=O). The carbonyl group creates a polar region on GAC's surface, allowing it to interact with polar molecules, such as ethanol, through various intermolecular forces, including hydrogen bonding and dipole–dipole interactions. A GAC's surface is usually complex and can contain various oxygen

functional groups, including carbonyl, carboxyl (-COOH), and hydroxy groups (-OH). These functional groups collectively contribute to the adsorption capabilities of GAC, but carbonyl groups are particularly effective at adsorbing polar molecules because of their strong dipole moments [53]. Elements such as nitrogen, phosphorus, or sulfur have not been detected on the surface of GACs.

3.2. Adsorption–Desorption Experiments

The ethanol content in the gas phase was determined based on calculations from the calibration curve. The ethanol content was related to the value of y_{EtOH} and φ_{EtOH} in SS. In this section, the y_{EtOH} values are based on those obtained in Section 2.3. The theoretical background of the ethanol content and the y_{EtOH} values obtained based on calculations from the calibration curve were compared. The results are presented in the graph in Figure 5.
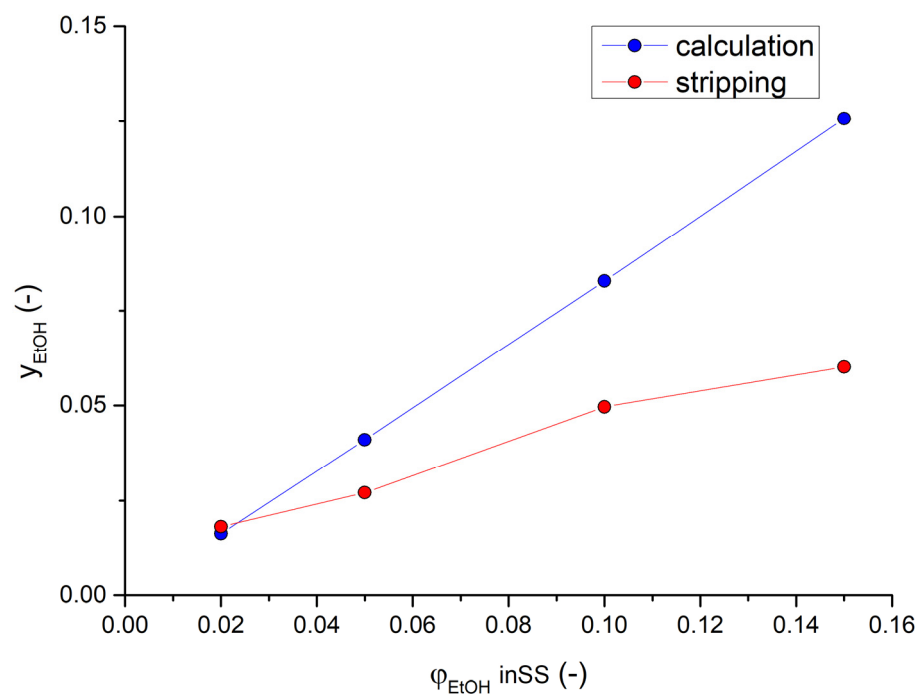

Figure 5. Graphical dependence of the molar fraction in the gaseous phase determined by calculation of the equilibrium state and by calculation based on the calibration curve for stripped SS.

From the graph in Figure 5, it is clear that the y_{EtOH} values obtained by calculation from the equilibrium state are higher than the y_{EtOH} values obtained experimentally during the stripping of SS. This is because, during stripping, the gas does not have enough time to reach an equilibrium state. The only exception in this case is SS, with a concentration of 2% *v/v*. It is clear from the graph that, by stripping, approximately the same ethanol concentration is achieved in both the gas and liquid phases. Even though the value of y_{EtOH} above SS is lower than in the equilibrium state (in cases 5, 10, and 15% *v/v* SS); this does not affect the efficiency of the transition of the substance from liquid to gas or the generation of gas containing ethanol intended for adsorption. It is also important to mention that the stripping gas has the function of a "transfer medium", i.e., it is the driving force for the transfer of the substance through the adsorption–desorption device. The high efficiency of ethanol's removal from fermentation broth using stripping is also described in the publication by Krings et al. [28]. The authors found that stripping can effectively remove ethanol from the fermentation broth to the extent that it does not inhibit the yeast that is present and promotes ethanol production. The same problem was dealt with by a group of authors in the publication by Hashi et al. [54] (the use of fermentation broth

stripping for ethanol separation), who found that the use of this method is highly effective and prospective.

The adsorption of ethanol on GAC took place through the gradual desorption of ethanol from SS. With the process conditions mentioned above, the entire adsorbent bed (GAC) was gradually saturated with adsorbate. The adsorption of ethanol on GAC was accompanied by an exothermic effect [23]. The exothermic effect adsorption of the gas phase was recorded by eight thermocouples located in the adsorption column. Based on the progress of the temperature field, the position of the adsorption zone (the mass transfer zone) could be roughly estimated [3]. In Table 2, the results of the main adsorption–desorption experiments for all three kinds of chosen GAC are listed.

Table 2. Summarized main results of adsorption–desorption experiments.

	GAC1	GAC2	GAC3
c_{SS} (%)	c_p (%)	c_p (%)	c_p (%)
2	19.97 ± 1.05	17.52 ± 3.44	15.46 ± 2.80
5	36.50 ± 2.60	39.08 ± 1.05	36.88 ± 2.70
10	47.79 ± 2.59	52.25 ± 0.99	52.27 ± 2.34
15	52.25 ± 0.50	57.42 ± 1.53	58.42 ± 0.55

The first column of Table 2 shows the ethanol concentration in SS (at the beginning of the separation process), and the values of ethanol concentration in the separation product (mean ± SD) are shown in the other columns. From the results listed in Table 2, it is clear that the ethanol concentration in the product increases when the ethanol concentration in SS increases. On the other hand, the enrichment factor of the separation decreases with an increased ethanol concentration in SS. Similar results are published in an article by Oumi et al. [48], where the authors studied the adsorption of binary gas mixtures (ethanol/water) onto silicate at 27 °C with different crystallinity. The authors observed that ethanol molecules preferentially adsorb on silicalite with fewer structure defects.

Figure 6 shows the adsorption–desorption results of experiments with chosen types of granulated activated carbons (GAC1–GAC3) with deviations. The highest value of ethanol concentration in the product of the separation process for 2% SS had a GAC1; ethanol concentration in the product is, on average, 20% *v/v* of ethanol. Although GAC1 has the smallest specific surface (736.12 m^2/g), the concentration of ethanol in the separation product was the highest at 2% *v/v* SS. On the contrary, using GAC3 with the highest surface area value (1025.97 m^2/g) resulted in a product with the lowest ethanol concentration. This phenomenon was due to the oxygen content of the GAC surface, which is discussed below. Using the SS with an ethanol concentration of 5% *v/v* and the separation process, the product with the highest ethanol concentration was acquired using GAC3; the product had an average ethanol concentration of 39% *v/v*. With an SS of 10% *v/v*, the product with the highest ethanol content of 52.3% *v/v* was obtained by the separation process using GAC2 and GAC3 (in both cases, the same average value of ethanol concentration). The SS with an ethanol concentration of 15% *v/v* could be concentrated to an average of 58.4% *v/v* ethanol by the separation process in our device (the highest value of ethanol concentration in the product was 59.0%, with GAC3 as the adsorbent. The experimental results obtained by us correlate with the results published by Cho and Hwang [36]. From the results above, it is possible to state the high efficiency of our chosen separation process in terms of concentrating the present volatile organic compound, ethanol, as the primary product of the fermentation process. The efficiency of the separation, the enrichment factor, is thus, for aqueous solutions of ethanol, up to 10 times the initial ethanol concentration (i.e., the concentration of ethanol in the separation product was 10 times higher than that in the stock solution). From the experiments performed, the total deviation in the ethanol gain in the separation product was at the level of 1.8%, the smallest deviation value was 0.5%, and the highest was 3.4%. From the above, we can see that the repeatability of the

experiments was high, even though granulated activated carbon was used repeatedly. The regeneration of the GACs was carried out in a laboratory oven at a temperature of 200 °C until the moisture value was ≤2%. The moisture determination was provided using a moisture-analyzer VWR International, MB 60 (Randor, PA, USA). The temperature program for the moisture determination was set up for 20 min at a temperature of 180 °C. The set temperature was chosen so that the adsorbed adsorbate (gaseous phase with water and ethanol) was removed from the GACs as efficiently as possible. No reduced efficiency of ethanol separation was observed with the repeated use of GAC. This phenomenon is described in a publication by Li et al. [2].
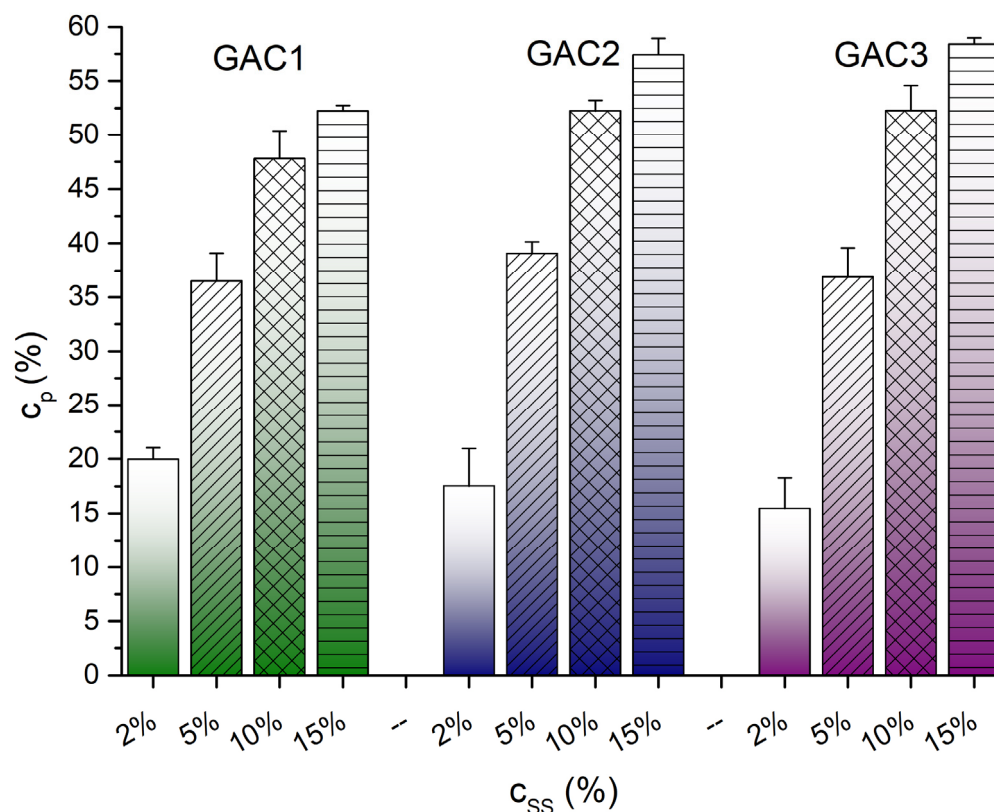

Figure 6. Graph of the major adsorption–desorption results, showing the ethanol concentration in the SS related to the ethanol concentration in the product.

In Section 3.1, showing the characterization of the GACs' surface, there is a certain correlation between the oxygen content on the surface of the GAC and ethanol adsorption. This fact is confirmed by the results of the separation experiments. With the zero/low oxygen content on the GAC surface, a high separation efficiency was observed at the low ethanol concentration in SS (2% *v/v*). A significant influence of the oxygen on the surface of the GAC was observed with a 2% stock solution and the GAC1 as adsorbent, despite the fact that the surface area of GAC1 had the lowest value and oxygen was not detected on the surface. By increasing the ethanol concentration in SS, this effect decreased; however, the high value of the surface area of GAC begins to play a significant role. From the results of the experiments with an ethanol concentration of 10 and 15% *v/v* in SS, it was possible to observe an almost identical value of ethanol in the separation product precisely because of the influence of oxygen on the surface of the GAC, despite the fact that the difference in the surface area of GAC2 and GAC3 was approximately 100 m^2/g. Both parameters (oxygen content on the GAC surface and surface area) had the same trend in influencing the concentration effect, as is clear in the graph in Figure 7.
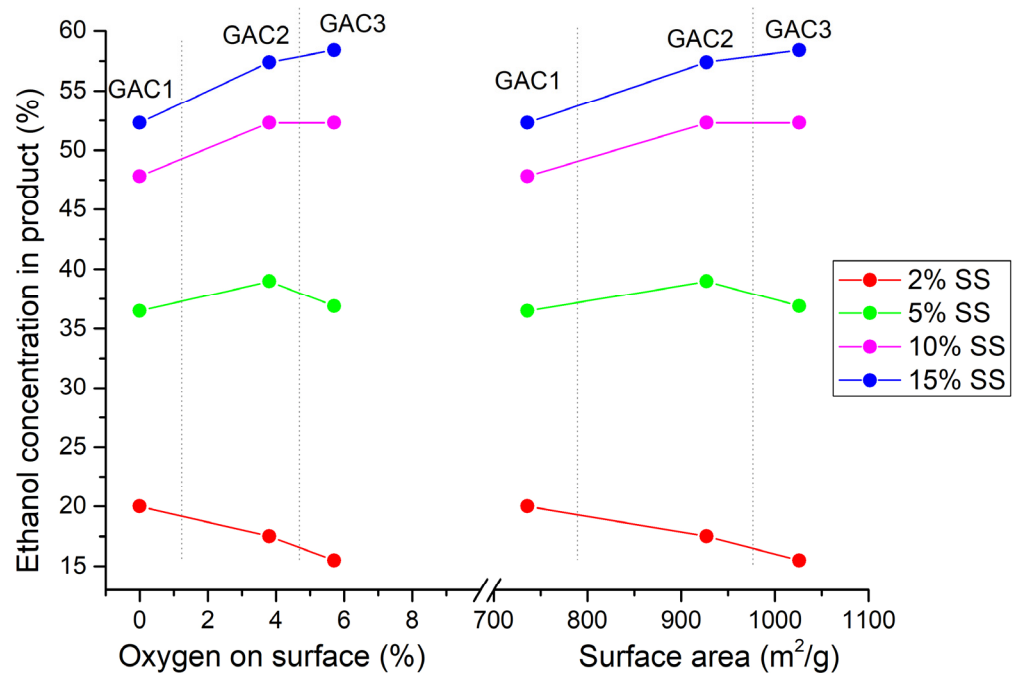
Figure 7. Relationship among the content of the oxygen on the GAC's surface, specific surface area values, and the ethanol concentration in the product for different ethanol concentrations in SS.

3.3. Adsorption–Desorption Mathematical Model

To create a mathematical model describing the concentration of the stock solution with a different ethanol concentration using the adsorption process, it was necessary to find the dependence of the process parameters and parameters of the individual sorbents on the ethanol content in the product of the experiments. Such parameters include the specific surface area value, pore radius, sorbent particle size, ethanol amount in the stock solution, and its input concentration. Dependencies among physical quantities can be replaced by dependencies among dimensionless arguments–criteria. The creation of dimensionless criteria will ensure the unit uniformity of the created mathematical model. The concentration ratio of the mixture was chosen as the first dimensionless criterion. This ratio is given by the ratio between the ethanol concentration in the product, c_p, and ethanol concentration in the stock solution, c_{SS} (at the beginning of the adsorption process). Figure 8 shows the dependence between these two process parameters.

From Figure 8, it is clear that it is possible to determine the relationship between these two parameters described by the power function with the high value of the determination coefficient. The trend line describes the decreasing trend of the enrichment factor at a higher ethanol concentration in SS.

The next dimensionless criteria contain a specific surface area, SA, particle size, d, and average pore size, d_p, of the chosen GACs. The median particle size, determined through image analysis using PartAn 3D, was chosen as the characteristic diameter for size. The median, unlike the average value, is not affected by extreme values of the particle size. Another parameter of this criterion is the ethanol mass, m, used for mixing the stock solution with a needed concentration, c_{SS}. The aim was to obtain a relationship between the concentration ratio as a function of other process parameters according to Equation (5):

$$\frac{c_p}{c_{SS}} = f\left(\frac{SA.m}{d.d_p}\right),\tag{5}$$

For the approximation of nonlinear dependencies, a program was created using the software Mathematica 8 (Wolfram, IL, USA). The NonLinearModelFit function was used

to determine the functional dependencies among individual criteria. The power model presented in Equation (6) performed best in the tests.

$$\frac{c_p}{c_{SS}} = A \times \left(\frac{SA.m}{d.d_p} \right)^B + C,$$ (6)

where A, B, and C are model parameters. The coefficients A and C determine the shift in the model, and coefficient B is the power of the function. The values of these parameters for each GAC are shown in Table 3. The accuracy of the mathematical model is shown in Figure 9.
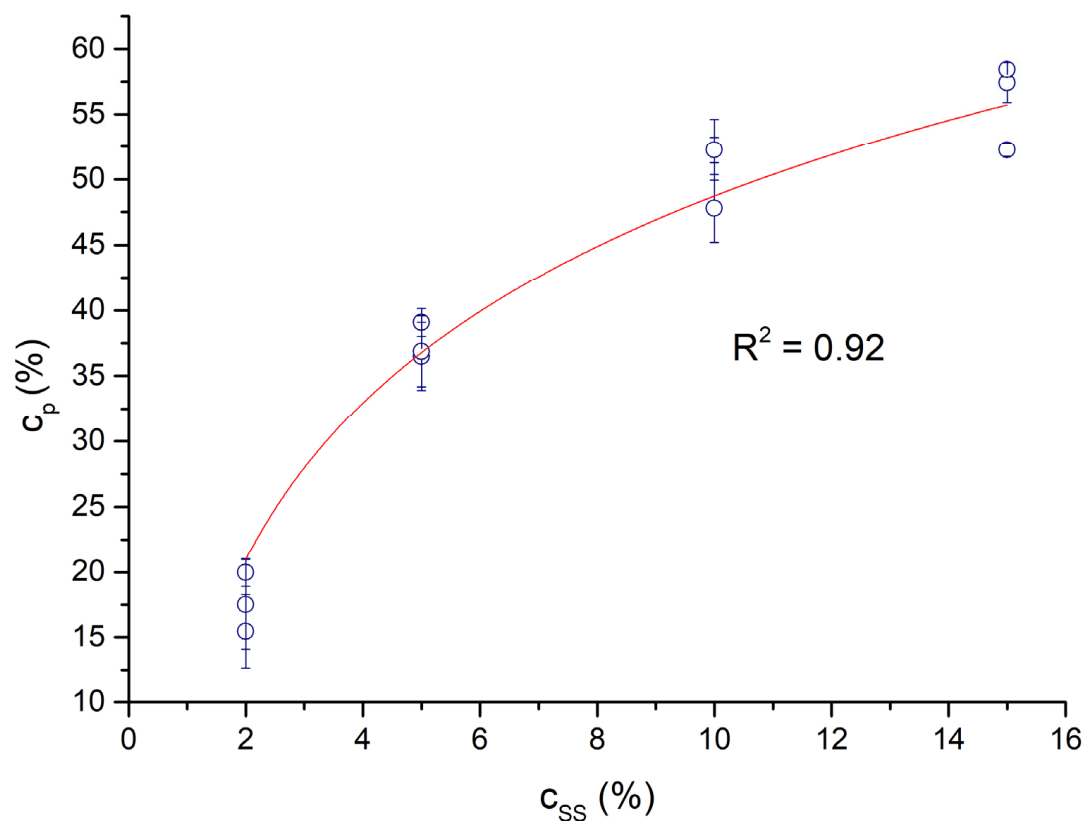

Figure 8. Graphical dependence between the ethanol concentration in SS and the ethanol concentration in the product of the separation process. The circles represent the mean value and standard deviation of repeated experiments; the red line represents the fitting using a power function.

Table 3. Summarized model parameters A, B, and C and the coefficient of determination.

GAC	Model Parameter			R^2
	A	B	C	
GAC1	-124.549	0.0175	193.018	0.9983
GAC2	-2.272×10^{-3}	0.353	15.091	0.9952
GAC3	-8.698×10^{-4}	0.382	12.901	0.9978

In the graph in Figure 9, the circles represent individual experiments; the red, dashed line represents $x = y$ (c_p predicted $= c_p$ measured); and the blue, dotted lines represent the interval for 95% of the results.
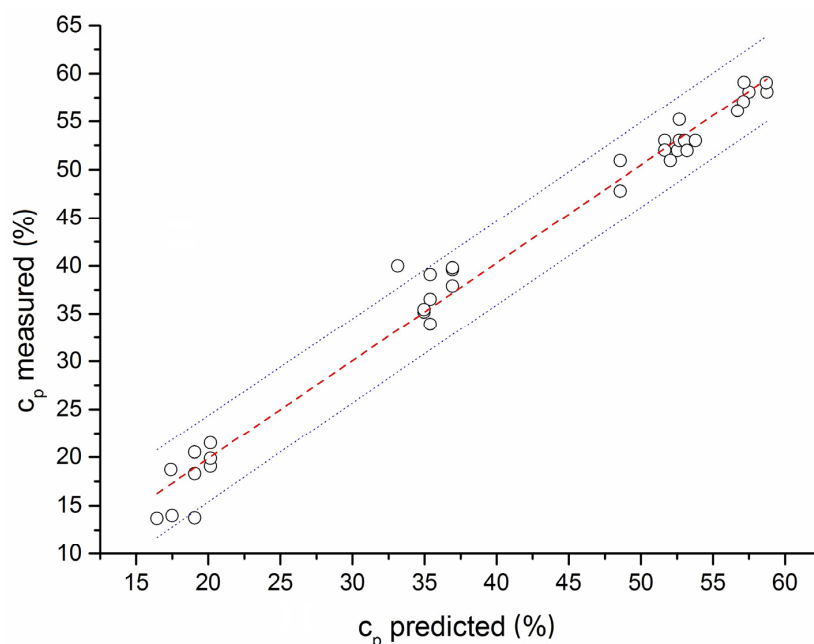
Figure 9. Experimental and predicted data obtained by our mathematical model for ethanol concentration in the separation product. The circles represent individual experiments; the red, dashed line represents *x* = *y*; and the blue, dotted lines represent the interval for 95% of the results.

3.4. Ethanol Separation from Fermentation Broth

One of the many uses of our device is the continuous removal of ethanol during the fermentation process and its adsorption on the adsorbent. Our idea was to increase the efficiency of ethanol production (our device was patented). The newly developed device needed to be tested with the real matrix: fermentation broth from apples. The fermentation broth was prepared from no specified variety of apples. The fermentation process took place for 9 days at laboratory temperature. After 9 days, the fermentation broth was pumped into our adsorption–desorption device where VOCs were separated. The separation conditions were the same as in the experiments with the aqueous ethanol mixture. In the fermentation broth, the concentration of selected saccharides and ethanol was determined every day during the fermentation process using the GC-FID, as described in Section 2. Ethanol in the separation product was also determined by GC-FID as is described in the Materials and Methods section. The fermentation process, which was accompanied by a decrease in sugar content and an increase in ethanol content, is shown in Figure 10.

From the graph in Figure 10, it is clear that, during fermentation, the present saccharides were gradually converted into ethanol, the primary product of fermentation. The determination of saccharides and ethanol was carried out as described in Section 2.2 (Materials and Methods). The analysis of the liquid sample was carried out with GC-FID. Very similar results (decrease in sugar content and increase in the ethanol content during fermentation) are presented in other publications [31,55,56].

From the graph in Figure 11, it is clear that there was a significant change in the ethanol concentration. The chromatographic records compare the response (concentration) of ethanol before the adsorption–desorption (separation) process and after the separation process. The initial ethanol concentration was 0.65%. After the adsorption–desorption process, the ethanol concentration in the separation product was 11.35%. The enrichment factor of the separation efficiency with a real sample (fermentation broth) was almost 18 times. For the real sample experiment, GAC3 was chosen as the adsorbent because it has the highest surface area value. This parameter was evaluated as one of the most important in terms of the adsorption of VOCs that are present in the fermentation broth. After the separation process, it was possible to observe the adsorption of the apple aroma on the used GAC3, while the presence of an apple aroma could be detected by the nose. The adsorbed

apple aroma is possible to separate from GAC, for example, by washing with hot steam or extraction with an organic solvent [28,57]. The biggest advantage of this separation process is that it is not necessary to heat (bring to boil) a mixture that contains ethanol (stock solution and fermentation broth, respectively). This fact is important because after the ethanol is separated from the fermentation broth, the further production of ethanol is possible from the yeasts that are present and have not been killed by the high temperature [25,31,35,37].
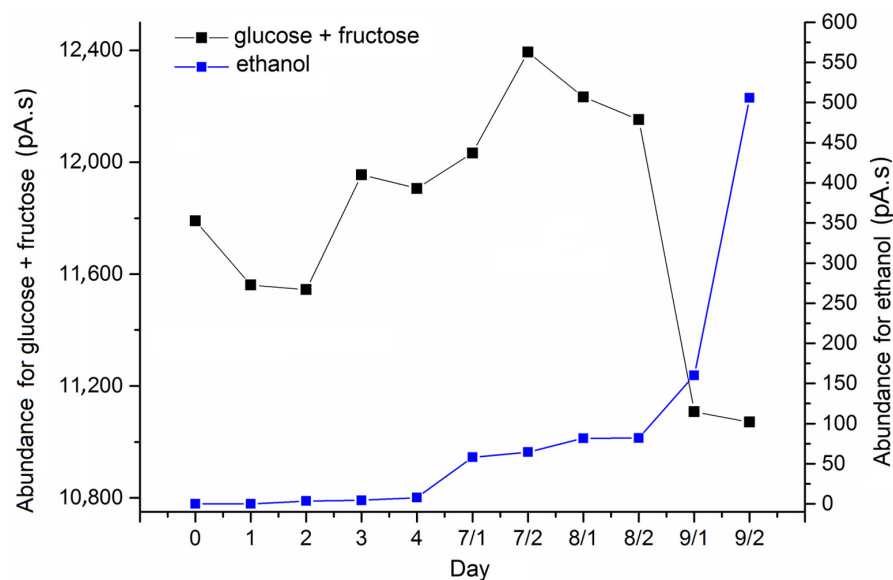

Figure 10. The GC-FID determination of glucose + fructose and ethanol in fermentation broth during the fermentation process.
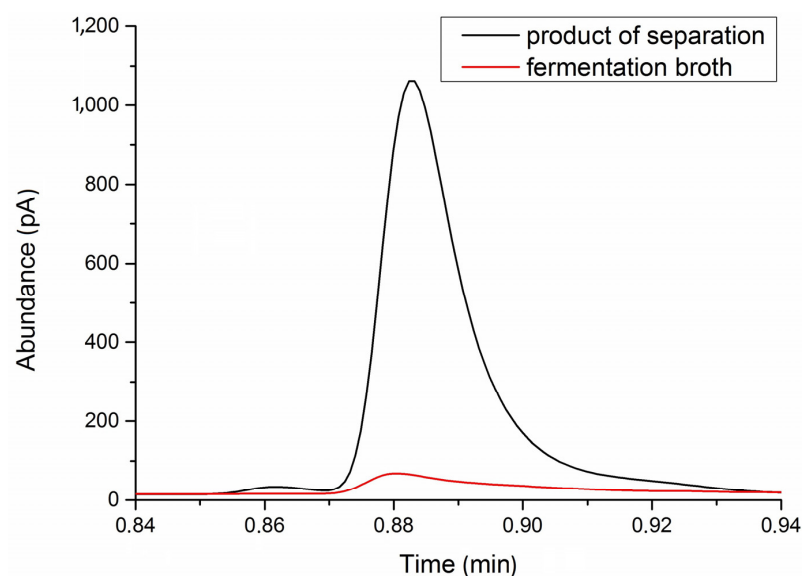

Figure 11. GC-FID chromatogram of ethanol content in fermentation broth (before the separation process) and in product (after the separation process).

4. Conclusions

Our separation device, which uses four basic processes (adsorption, desorption, stripping, and condensation), achieves high enrichment factor values for ethanol separation. The separation experiments were performed with the device using a model solution with different values of ethanol concentration (2, 5, 10, and 15% *v/v*) and the real matrix (fermentation broth). Each of the experiments were repeated three times, and the experiments had a high level of repeatability because the average deviation in the obtained ethanol concentration

in the separation product was only 1.8% *v/v*. Using SS with an ethanol concentration of 2% *v/v*, the enrichment factor was equal to 10. As the ethanol concentration in SS increases, the enrichment factor decreases, but the concentration of ethanol in the separation products also increases. The separation experiments with fermentation broth prove the applicability of our device for a real matrix. The initial ethanol concentration in the fermentation broth was 0.65%, but using our separation device, a product with an ethanol concentration of 11.35% was acquired, which indicates an enrichment factor of 18. With our separation device, it is possible to effectively remove ethanol from the fermentation broth at room temperature. The separation and production of ethanol can, thus, be continuous, and it is possible to produce much more ethanol from one batch than with commonly used separation devices, which makes our device unique. The mathematical model designed by us predicts the ethanol concentration in the product with high accuracy. Our mathematical model takes into account the surface area of GAC, GAC particle size, GAC pore diameter, amount of ethanol in SS, and ethanol concentration in SS.

5. Patents

Our newly developed adsorption–desorption device is patented by the Industrial Property Office of the Slovak Republic with Application Number: 288853.

Author Contributions: Conceptualization, investigation, methodology, writing—original draft, and formal analysis, Ľ.G. and O.M.; investigation, M.J., Z.G. and I.V.; investigation, conceptualization, and visualization, J.K. and J.B.; methodology, R.K. All authors have read and agreed to the published version of the manuscript.

Data Availability Statement: The data presented in this study are available upon request from the corresponding author. The data are not publicly available because of the extensive quantity of values.

Conflicts of Interest: The authors declare no conflict of interest.

Nomenclature

c_p	Ethanol concentration in the product (%)
c_{SS}	Ethanol concentration in stock solution (%)
d	Particle size (m)
d_p	Pore average size (m)
GAC	Granulated activated carbon
GC − FID	Gas chromatography with flame ionization detector
m	Ethanol mass in SS (g)
n_i	Amount of substance i (mol)
n_{total}	Sum of the amount of substances in system (mol)
p_i	Partial pressure of component i (kPa)
p_i°	Vapor pressure of component i (kPa)
p_{total}	Total pressure above SS (kPa)
r_p	Pore average radius (nm)
SA	Surface area (m^2/g)
SD	Standard deviation (%)
SS	Stock solution
VOC	Volatile organic compound
V_p	Specific pore volume (cm^3/g)
y_{EtOH}	Molar fraction of ethanol in gas (-)
y_i	Molar fraction of component i in gas (-)
φ_{EtOH}	Volume fraction of ethanol (-)

References

1.　Abdehagh, N.; Dai, B.; Thibault, J.; Tezel, F.H. Biobutanol Separation from ABE Model Solutions and Fermentation Broths Using a Combined Adsorption—Gas Stripping Process. *J. Chem. Technol. Biotechnol.* **2016**, *92*, 245–251. [CrossRef]
2.　Li, X.; Zhang, L.; Yang, Z.; Wang, P.; Yan, Y.; Ran, J. Separation and Puri Fi Cation Technology Adsorption Materials for Volatile Organic Compounds (VOCs) and the Key Factors for VOCs Adsorption Process: A Review. *Sep. Purif. Technol.* **2020**, *235*, 116213. [CrossRef]
3.　Patel, H. Fixed-Bed Column Adsorption Study: A Comprehensive Review. *Appl. Water Sci.* **2019**, *9*, 45. [CrossRef]
4.　Delgado, J.A.; águeda, V.I.; Uguina, M.A.; Sotelo, J.L.; García, A.; Brea, P.; García-Sanz, A. Separation of Ethanol-Water Liquid Mixtures by Adsorption on a Polymeric Resin Sepabeads 207®. *Chem. Eng. J.* **2013**, *220*, 89–97. [CrossRef]
5.　Abdehagh, N.; Gurnani, P.; Corporation, T.; Tezel, F.H.; Thibault, J. Adsorptive Separation and Recovery of Biobutanol from ABE Model Solutions Adsorptive Separation and Recovery of Biobutanol from ABE Model Solutions. *Adsorption* **2015**, *21*, 185–194. [CrossRef]
6.　Qureshi, N.; Hughes, S.; Maddox, I.S.; Cotta, M.A. Energy-Efficient Recovery of Butanol from Model Solutions and Fermentation Broth by Adsorption. *Bioprocess Biosyst. Eng.* **2005**, *27*, 215–222. [CrossRef]
7.　Salvador, F.; Martin-Sanchez, N.; Sanchez-Hernandez, R.; Sanchez-Montero, M.J.; Izquierdo, C. Regeneration of Carbonaceous Adsorbents. Part II: Chemical, Microbiological and Vacuum Regeneration. *Microporous Mesoporous Mater.* **2015**, *202*, 277–296. [CrossRef]
8.　Zhang, W.; Li, G.; Yin, H.; Zhao, K.; Zhao, H.; An, T. Adsorption and Desorption Mechanism of Aromatic VOCs onto Porous Carbon Adsorbents for Emission Control and Resource Recovery: Recent Progress and Challenges. *Environ. Sci. Nano* **2022**, *9*, 81–104. [CrossRef]
9.　Zhu, X.; Fan, Z.; Zhang, X.F.; Yao, J. Metal-Organic Frameworks Decorated Wood Aerogels for Efficient Particulate Matter Removal. *J. Colloid Interface Sci.* **2023**, *629*, 182–188. [CrossRef]
10.　Laksmono, J.A.; Pangesti, U.A.; Sudibandriyo, M.; Haryono, A.; Saputra, A.H. IOP Conference Series: Earth and Environmental Science Adsorption Capacity Study of Ethanol-Water Mixture for Zeolite, Activated Carbon, and Polyvinyl Alcohol. *IOP Conf. Ser. Earth Environ. Sci.* **2018**, *105*, 12025. [CrossRef]
11.　Hashi, M.; Tezel, F.H.; Thibault, J. Ethanol Recovery from Fermentation Broth via Carbon Dioxide Stripping and Adsorption. *Energy Fuels* **2010**, *24*, 4628–4637. [CrossRef]
12.　Zhang, X.; Gao, B.; Creamer, A.E.; Cao, C.; Li, Y. Adsorption of VOCs onto Engineered Carbon Materials: A Review. *J. Hazard. Mater.* **2017**, *338*, 102–123. [CrossRef] [PubMed]
13.　Gil, R.R.; Ruiz, B.; Lozano, M.S.; Martín, M.J.; Fuente, E. VOCs Removal by Adsorption onto Activated Carbons from Biocollagenic Wastes of Vegetable Tanning. *Chem. Eng. J.* **2014**, *245*, 80–88. [CrossRef]
14.　Ledesma, B.; Román, S.; Álvarez-Murillo, A.; Sabio, E.; González, J.F. Cyclic Adsorption/Thermal Regeneration of Activated Carbons. *J. Anal. Appl. Pyrolysis* **2014**, *106*, 112–117. [CrossRef]
15.　Silvestre-Albero, A.; Silvestre-Albero, J.; Sepúlveda-Escribano, A.; Rodriguéz-Reinoso, F. Ethanol Removal Using Activated Carbon: Effect of Porous Structure and Surface Chemistry. *Microporous Mesoporous Mater.* **2009**, *120*, 62–68. [CrossRef]
16.　Bradley, R.H.; Smith, M.W.; Andreu, A.; Falco, M. Surface Studies of Novel Hydrophobic Active Carbons. *Appl. Surf. Sci.* **2011**, *257*, 2912–2919. [CrossRef]
17.　Wolak, E.; Vogt, E.B.; Szczurowski, J. Chemical and Hydrophobic Modification of Activated WD-Extra Carbon. *E3S Web Conf.* **2017**, *14*, 02033. [CrossRef]
18.　Figueiredo, J.L.; Pereira, M.F.R.; Freitas, M.M.A.; Órfão, J.J.M. Modification of the Surface Chemistry of Activated Carbons. *Carbon* **1999**, *37*, 1379–1389. [CrossRef]
19.　Barroso-Bogeat, A.; Alexandre-Franco, M.; Fernández-González, C.; Gómez-Serrano, V. FT-Ir Analysis of Pyrone and Chromene Structures in Activated Carbon. *Energy Fuels* **2014**, *28*, 4096–4103. [CrossRef]
20.　Petrovic, B.; Gorbounov, M.; Masoudi Soltani, S. Impact of Surface Functional Groups and Their Introduction Methods on the Mechanisms of CO_2 Adsorption on Porous Carbonaceous Adsorbents. *Carbon Capture Sci. Technol.* **2022**, *3*, 100045. [CrossRef]
21.　Fletcher, A.J.; Uygur, Y.; Mark Thomas, K. Role of Surface Functional Groups in the Adsorption Kinetics of Water Vapor on Microporous Activated Carbons. *J. Phys. Chem. C* **2007**, *111*, 8349–8359. [CrossRef]
22.　Liu, H.; Yu, Y.; Shao, Q.; Long, C. Separation and Puri Fi Cation Technology Porous Polymeric Resin for Adsorbing Low Concentration of VOCs: Unveiling Adsorption Mechanism and e Ff Ect of VOCs' Molecular Properties. *Sep. Purif. Technol.* **2019**, *228*, 115755. [CrossRef]
23.　Qi, N.; LeVan, M.D. Adsorption Equilibrium Modeling for Water on Activated Carbons. *Carbon* **2005**, *43*, 2258–2263. [CrossRef]
24.　Wilkins, N.S.; Rajendran, A.; Farooq, S. Dynamic Column Breakthrough Experiments for Measurement of Adsorption Equilibrium and Kinetics. *Adsorption* **2021**, *27*, 397–422. [CrossRef]
25.　Baeyens, J.; Kang, Q.; Appels, L.; Dewil, R.; Lv, Y.; Tan, T. Challenges and Opportunities in Improving the Production of Bio-Ethanol. *Prog. Energy Combust. Sci.* **2015**, *47*, 60–88. [CrossRef]
26.　Fletcher, A.J.; Yüzak, Y.; Thomas, K.M. Adsorption and Desorption Kinetics for Hydrophilic and Hydrophobic Vapors on Activated Carbon. *Carbon* **2006**, *44*, 989–1004. [CrossRef]
27.　Bowen, T.C.; Vane, L.M. Ethanol, Acetic Acid, and Water Adsorption from Binary and Ternary Liquid Mixtures on High-Silica Zeolites. *Langmuir* **2006**, *22*, 3721–3727. [CrossRef]

28. Krings, U.; Kelch, M.; Berger, R.G. Adsorbents for the Recovery of Aroma Compounds in Fermentation Processes. *J. Chem. Technol. Biotechnol.* **1993**, *58*, 293–299. [CrossRef]

29. Claessens, B.; Cousin-saint-remi, J.; Denayer, J.F.M. *Efficient Downstream Processing of Renewable Alcohols Using Zeolite Adsorbents*; Springer: Cham, Switzerland, 2020.

30. Walker, G.M.; Stewart, G.G. Saccharomyces Cerevisiae in the Production of Fermented Beverages. *Beverages* **2016**, *2*, 30. [CrossRef]

31. Henrique, G.; Ponce, S.F.; Moreira, J.; Santos, S.; Jesus, D.; César, J.; Miranda, D.C.; Maciel, R.; Ramos, R.; Andrade, D.; et al. Sugarcane Molasses Fermentation with in Situ Gas Stripping Using Low and Moderate Sugar Concentrations for Ethanol Production: Experimental Data and Modeling. *Biochem. Eng. J.* **2016**, *110*, 152–161. [CrossRef]

32. Ouzzine, M.; Romero-Anaya, A.J.; Lillo-Ródenas, M.A.; Linares-Solano, A. Spherical Activated Carbons for the Adsorption of a Real Multicomponent VOC Mixture. *Carbon* **2019**, *148*, 214–223. [CrossRef]

33. Hu, Z.; Zhang, H.; Zhang, X.F.; Jia, M.; Yao, J. Polyethylenimine Grafted ZIF-8@cellulose Acetate Membrane for Enhanced Gas Separation. *J. Memb. Sci.* **2022**, *662*, 120996. [CrossRef]

34. Wei, Y.; Zhao, T.; Wang, J.; Chen, Y.; Wang, Q.; Liu, X.; Zhao, Y. Ultramicroporous Carbon Molecular Sieve for Air Purification by Selective Adsorption Low-Concentration CO_2 and VOC Molecules. *Ind. Eng. Chem. Res.* **2023**, *62*, 7635–7641. [CrossRef]

35. Sonego, J.L.S.; Lemos, D.A.; Rodriguez, G.Y.; Cruz, A.J.G.; Badino, A.C. Extractive Batch Fermentation with CO_2 Stripping for Ethanol Production in a Bubble Column Bioreactor: Experimental and Modeling. *Energy Fuels* **2014**, *28*, 7552–7559. [CrossRef]

36. Cho, C.W.; Hwang, S.T. Continuous Membrane Fermentor Separator for Ethanol Fermentation. *J. Membr. Sci.* **1991**, *57*, 21–42. [CrossRef]

37. Ponce, G.H.S.F.; Miranda, J.C.C.; Alves, M.; Maria, R.M.; Maciel, R.; De Andrade, R.R.; Conto, L.C. De Simulation, Analysis and Optimization of an In Situ Gas Stripping Fermentation Process in a Laboratory Scale for Bioethanol Production. *Chem. Eng.* **2014**, *37*, 295–300. [CrossRef]

38. Seo, D.J.; Takenaka, A.; Fujita, H.; Mochidzuki, K.; Sakoda, A. Practical Considerations for a Simple Ethanol Concentration from a Fermentation Broth via a Single Adsorptive Process Using Molecular-Sieving Carbon. *Renew. Energy* **2018**, *118*, 257–264. [CrossRef]

39. Gabrišová, L.; Peciar, P.; Macho, O.; Juriga, M.; Galbavá, P.; Nižnanská, Ž.; Kubinec, R.; Valent, I.; Peciar, M. The Development of a New Adsorption-Desorption Device. *Acta Polytech.* **2020**, *60*, 455–461. [CrossRef]

40. Perry, R.H. *Perry's Chemical Engineering Handbook*; McGraw-Hill Inc.: New York, NY, USA, 2007.

41. Kwon, S.H.; Cho, D. A Comparative, Kinetic Study on Cork and Activated Carbon Biofilters for VOC Degradation. *J. Ind. Eng. Chem.* **2009**, *15*, 129–135. [CrossRef]

42. Bley, M.; Duvail, M.; Guilbaud, P.; Penisson, C.; Theisen, J.; Gabriel, J.; Dufrêche, J. Molecular Simulation of Binary Phase Diagrams from the Osmotic Equilibrium Method: Vapour Pressure and Activity in Water—Ethanol Mixtures. *Mol. Phys.* **2018**, *116*, 2009–2021. [CrossRef]

43. Waller, R.; Strang, T.J.K. Physical Chemical Properties of Preservative Solutions—1. Ethanol-Water Solutions. *Collect. Forum* **1996**, *12*, 70–85.

44. *13322-2: ISO 13322-2*; Particle Size Analysis—Imange Analysis Methods—Dynamic Image Analysis. International Organization for Standardization: Geneva, Switzerland, 2006.

45. *9276-6: ISO 9276-6*; Representation of Results of Particle Size Analysis—Descriptive and Quantitative Representation of Particle Shape and Morphology. International Organization for Standardization: Geneva, Switzerland, 2008.

46. Faisal, A.; Zhou, M.; Hedlund, J.; Grahn, M. Recovery of Butanol from Model ABE Fermentation Broths Using MFI Adsorbent: A Comparison between Traditional Beads and a Structured Adsorbent in the Form of a Film. *Adsorption* **2016**, *22*, 205–214. [CrossRef]

47. Pellenz, L.; de Oliveira, C.R.S.; da Silva Júnior, A.H.; da Silva, L.J.S.; da Silva, L.; Ulson, S.M.D.A.G.; de Souza, A.A.U.; Borba, F.H.; da Silva, A. A Comprehensive Guide for Characterization of Adsorbent Materials. *Sep. Purif. Technol.* **2023**, *305*, 122435. [CrossRef]

48. Oumi, Y.; Miyajima, A.; Miyamoto, J.; Sano, T. Binary Mixture Adsorption of Water and Ethanol on Silicalite. In *Proceedings of the Studies in Surface Science and Catalysis*; Elsevier: Amsterdam, The Netherlands, 2002; Volume 142, pp. 1595–1602.

49. Thommes, M.; Kaneko, K.; Neimark, A.V.; Olivier, J.P.; Rodriguez-Reinoso, F.; Rouquerol, J.; Sing, K.S.W. Physisorption of Gases, with Special Reference to the Evaluation of Surface Area and Pore Size Distribution (IUPAC Technical Report). *Pure Appl. Chem.* **2015**, *87*, 1051–1069. [CrossRef]

50. Okolo, G.N.; Everson, R.C.; Neomagus, H.W.J.P.; Roberts, M.J.; Sakurovs, R. Comparing the Porosity and Surface Areas of Coal as Measured by Gas Adsorption, Mercury Intrusion and SAXS Techniques. *Fuel* **2015**, *141*, 293–304. [CrossRef]

51. Kazak, O.; Ramazan Eker, Y.; Bingol, H.; Tor, A. Preparation of Activated Carbon from Molasses-to-Ethanol Process Waste Vinasse and Its Performance as Adsorbent Material. *Bioresour. Technol.* **2017**, *241*, 1077–1083. [CrossRef]

52. Chen, X.; Jeyaseelan, S.; Graham, N. Physical and Chemical Properties Study of the Activated Carbon Made from Sewage Sludge. *Waste Manag.* **2002**, *22*, 755–760. [CrossRef]

53. Bansal, R.C.; Goyal, M. *Activated Carbon Adsorption*; CRC: Boca Raton, FL, USA, 2005.

54. Hashi, M.; Thibault, J.; Tezel, F.H. Recovery of Ethanol from Carbon Dioxide Stripped Vapor Mixture: Adsorption Prediction and Modeling. *Ind. Eng. Chem. Res.* **2010**, *49*, 8733–8740. [CrossRef]

55. Tronchoni, J.; Gamero, A.; Arroyo-lópez, F.N.; Barrio, E.; Querol, A. International Journal of Food Microbiology Differences in the Glucose and Fructose Consumption pro Fi Les in Diverse Saccharomyces Wine Species and Their Hybrids during Grape Juice Fermentation. *Int. J. Food Microbiol.* **2009**, *134*, 237–243. [CrossRef]

56. Berthels, N.J. Discrepancy in Glucose and Fructose Utilisation during Fermentation by Saccharomyces Cerevisiae Wine Yeast Strains. *FEMS Yeast Res.* **2004**, *4*, 683–689. [CrossRef]

57. Taylor, P.; Nongonierma, A.; Voilley, A.; Cayot, P.; Quéré, L.; Springett, M.; Springett, M.; Voilley, A. Mechanisms of Extraction of Aroma Compounds from Foods, Using Adsorbents. Effect of Various Parameters. *Food Rev. Int.* **2006**, *22*, 51–94. [CrossRef]